

# Hardware Efficient Approximate Convolution with Tunable Error Tolerance for CNNs

Vishal Shashidhar<sup>1</sup>, Anupam Kumari<sup>2</sup>, Roy P. Paily<sup>3</sup>

Department of Electrical and Electronics Engineering

Indian Institute of Technology Guwahati

Email: v.shashidhar@iitg.ac.in<sup>1</sup>, a.kumari@iitg.ac.in<sup>2</sup>, roypaily@iitg.ac.in<sup>3</sup>

*Abstract*—Modern Convolutional Neural Networks (CNNs) are increasingly power-intensive and computationally heavy, posing significant challenges for deployment on resource-constrained edge devices. While current research often exploits “hard” sparsity by skipping mathematical zeros, these methods are inherently limited because the fraction of mathematical zero values decreases significantly in deeper feature maps. While ReLU activations typically produce a zero fraction of only 20–50% in these layers, smooth activation functions like Tanh generate virtually no zeros at all, rendering traditional skipping techniques ineffective. This paper proposes a “soft sparsity” paradigm that utilizes a novel hardware-efficient approximation strategy to selectively omit multiplications whose contributions to the final output are negligible, even if they are non-zero. The method leverages the Most Significant Bit (MSB) as a low-cost hardware proxy for logarithmic magnitude, allowing the system to compare relative product sizes against a tunable threshold without explicitly performing the multiplication. Integrated as a custom instruction within a 32-bit RISC-V processor, this approach was evaluated using the LeNet-5 architecture on the MNIST dataset. Results demonstrate that for ReLU-based models, inference can be performed by reducing no. of MACs by 88.42% with no loss in accuracy. Furthermore, the method remains effective for smoother activations like Tanh, which lack hard zeros, achieving a reduction of 74.87% of total multiplications while maintaining full accuracy. This translates to a 5x reduction in number of multiplication operations when compared to traditional hard-zero skipping paradigms. As a consequence of this reduction in multiplication operations that have to be performed, inactive multipliers can be clock gated to conserve power. Power reduction will be sub linear to the reduction in multiplications as prior work has indicated memory access to also be a large contributor to power consumption during convolution. We estimate power reductions of 35.2% and 29.96% per inference operation of LeNet-5 using ReLU and Tanh activations respectively.

*Index Terms*—CNN, Approximate Convolution, Sparsity, Soft Sparsity, Tunable Error Tolerance, RISC-V, Custom Instruction, MAC Operation Reduction, LeNet-5, MNIST, Activation Functions (ReLU, Tanh)

## I. INTRODUCTION

CNNs excel at identifying spatial patterns which has found a large variety of applications including object classification in images, facial recognition, NLP tasks and structured signal analysis. CNNs are composed of convolutional layers, activation layers which perform a non-linear function on the neurons, pooling layers responsible for down-sampling and fully connected layers which flattens 2D feature maps into a 1D

TABLE I: Parameter Count and Computational Cost of Popular CNN Architectures

Architecture	Layer Type	# Parameters	# Operations (FLOPs)
LeNet-5	Conv	~3k	~300k
	FC	~58k	~60k
AlexNet	Conv	~3.7M	~650M
	FC	~58.6M	~58M
ResNet-50	Conv	~23.5M	~3.8G
	FC	~2M	~2M
GoogLeNet	Conv	~5.7M	~1.5G
	FC	~1M	~1M

vector and connects every input of the layer to every output of the layer. The values of the filter matrices for the convolution layers and the weights of the FC layer are the parameters which are set and stored during training. Convolutional layers account for the vast majority of arithmetic MAC (multiply and accumulate) operations sometimes accounting for over 99% of FLOPs (floating point operations) such as in ResNet-50 while representing negligible fraction of the model’s parameters [12] while Fully Connected layers dominate the model’s memory footprint due to the dense interconnections[13], however, modern architectures like ResNet and GoogLeNet mitigate heavy FC layers, shifting the parameter distribution more toward convolution and global pooling[14].

Modern CNNs are increasingly becoming bulkier and have billions of MAC operations making it power intensive and unsuitable for edge devices, while also containing redundancy in the form of Sparsity where there are large fractions of zero or close to zero values in input matrices and weights whose activation have negligible contribution to the output. In CNN workloads, input sparsity varies widely by application. Natural images (e.g., ImageNet, CIFAR) are largely dense, with less than 5% exact zeros, though 20–50% of pixels may be near-zero in smooth background regions. Handwritten or binary-like inputs (e.g., MNIST, document images) exhibit 60–90% zero or near-zero pixels. In circuit and EDA applications—such as netlist adjacency matrices, routing congestion maps, and placement grids—input tensors are often 80–99% sparse, reflecting localized connectivity and activity. Event-based vision, remote sensing, and scientific grids typically show 70–95% sparsity, often spatially clustered.

In literature, this sparsity has been exploited in primarily

two ways, the first being pruning weights which have a negligible contribution to the output and the second by skipping the computation of MAC operations when the input activation is 0. These do not directly lead to reduction in number of cycles required as in modern hardware MACs are executed in parallel, which means that even though an operation is skipped, that thread will have to wait for the completion of execution of parallel threads before proceeding to the next operation. Specialized hardware relies on storing only the non-zero values in CSR (compressed sparse row) format or CSC (Compressed Sparse Column) format and accessing elements via indexing, but this results in substantial control and power overhead.

However, the power consumption can be brought down by clock gating a multiplier when a MAC operation need not be performed. Prior research has shown that the dominant factor in power consumption is data access and not MAC operations, hence energy savings are sub-linear with respect to operation reduction. Han et al. [1] reported 3-5 pJ per 32-bit MAC operation and 5-10 pJ per 32-bit SRAM access for 45nm technology, meaning that reducing MAC operations by 100% will result in power reduction by about 25-50% if corresponding memory access is not optimized, assuming data present in SRAM. K. Guo et al. [16] reported that typical energy for a 32-bit SRAM access costs twice as much as 32-bit multiplication for 22nm technology, implying 100% MAC reduction would result in about 33% power reduction. Chen et al. [10] achieved a 45% power consumption reduction by zero skipping at 65 nm technology. DRAM access costs multiple orders of magnitude greater than either SRAM access or MAC operation.

Early literature focused on static weight sparsity in FC layers, Han at el. [1] proposed a 3-stage train-prune-retrain pipeline that compresses neural networks by removing weights with magnitudes below a heuristic threshold, followed by iterative fine-tuning to recover lost accuracy. However, these static methods are inherently limited because they cannot adapt to the "dynamic sparsity" that arises from specific input data and requires specialized hardware such as Cambricon-X [17] to achieve speedup where the control and indexing cost contribute to a 30-35% power overhead.

To capture this input-dependent redundancy, researchers developed dynamic accelerators such as Cnvlutin [4] and NullHop [5], which employ runtime zero-skipping to bypass multiplications involving activations nullified by the ReLU function. However, If ReLU activation function is not used then there will be no zero values in subsequent feature maps and even when used the fraction of pixel values forced to zero by ReLU may not always be significant, we found that it is 20-50% per layer for MNIST images, which typically have an 80% input sparsity, on the LeNet architecture with fewer zeros appearing in deeper layers. these designs are often hampered by the rigid binary nature of "hard" zeros, incurring significant metadata overhead and load imbalance [8] while still being forced to execute any multiplication where both operands are even slightly non-zero. While advanced dual-side architectures like Sparch [9] and predictive frameworks like SnaPEA [11]

attempt to bridge these gaps by identifying ineffectual neurons before they are fully processed, they remain tethered to the assumption that only a mathematical zero can be safely ignored. This research introduces a more flexible "soft sparsity" paradigm, proposing custom hardware that dynamically evaluates the product of a weight and an activation against a tunable threshold without explicitly computing the product. By skipping computations that fall below this significance level, regardless of whether they are exactly zero, this approach allows for a more aggressive exploitation of data redundancy. This is achieved without any control or indexing overheads and without having to modify the neural network by cycles of pruning and retraining.

This paper is organized as follows: Section II explains the background and motivation behind `conv_approx()`, the novel approximation operation that we introduce. Section III explains the algorithmic principle of using the Most Significant Bit (MSB) as a low-cost hardware proxy for logarithmic magnitude to identify and omit insignificant products. Section IV details the hardware implementation, specifically the integration of a custom `conv_approx()` instruction into a 32-bit RISC-V processor using a specialized 5-stage Finite State Machine (FSM). Finally, Section V provides a comprehensive error and performance analysis using the LeNet-5 architecture on the MNIST dataset. The primary contributions include a novel hardware-efficient approximation algorithm with a tunable error-tolerance mechanism for balancing accuracy and efficiency, and the demonstrated ability to reduce MAC operations by up to 88.42% for ReLU and 74.87% for Tanh activations during LeNet-5 inference with negligible impact on accuracy.

## II. BACKGROUND

The output of each individual convolution between a feature map and a filter matrix can be written as a matrix where each cell is given by a sum of products. For an output location (i,j),

$$Y(i, j) = \sum_{r=0}^{k-1} \sum_{s=0}^{k-1} X(i+r, j+s) K(r, s) \quad (1)$$

Current literature only skips computation if activation is a mathematical zero, however there may exist cases where a particular product in a sum of products is insignificant relative to other products. This may be because the activation or weight is relatively small or because there is another product term which is dominating over the rest. In such cases we can skip the computation of product terms which have an insignificant contribution to the sum. The output will not be the exact mathematical value, but the objective of convolutional layers is to identify spatial patterns, and numerical accuracy can be traded for reduction in computational operations as long as the accuracy of the final output is not compromised.

We can intuitively see cases where some products will dominate over the others such as when the filter overlaps against an edge in the feature map, some weights will correspond to high activation values and will likely have large products

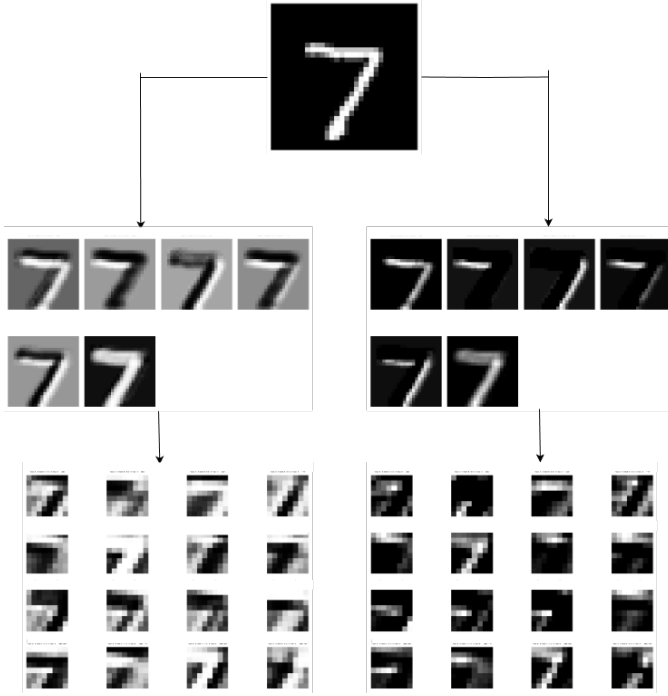


Fig. 1: Left and right side show subsequent feature maps with Tanh and ReLU activation respectively.

whereas some weights will correspond to low activation values and will likely have products which are insignificant relative to the former products, in such a case the multiplication of the weights and activations whose products are insignificant can be skipped. We will elaborate how we decide whether a multiplication can be skipped without explicitly calculating the product in a later section.

The decision regarding skipping computation of certain products is taken after considering both activation and weight, as such a decision taken after considering only either one may lead to the decision being incorrect. This method allows us to robustly skip many more computations than just zero-skipping paradigms. Current zero skipping algorithms operate on inputs and subsequent feature maps after application of ReLU activation function, which is basically  $f(X) = \max(0, X)$ . ReLU sets all negative pre-activations to exactly zero, so the neuron stops distinguishing between “slightly negative” and “very negative” inputs in that region. This can remove potentially useful contrast information (e.g., weak vs strong inhibition signals), which might reduce representational capacity compared with smooth or signed activations. Using Techniques like Ke initialization, batch normalization and residual connections keep activations from collapsing into the negative half line, due to which ReLU-based networks match smoother activations on many vision and language benchmarks. Leaky ReLU, PReLU, and ELU keep a small negative slope, so negative inputs are not completely discarded, and gradients remain nonzero for all inputs. These variants often show modest but consistent gains. Our algorithm performs pruning

on further feature maps without being conditioned on having to use ReLU activation function as it is not dependent on having hard zeros to skip MAC operations.

### III. ALGORITHMIC PRINCIPLE AND WORKING

Each element of the output feature map produced by a convolution operation is computed as a weighted sum of input values, i.e., a sum of pairwise products. This work proposes an approximation strategy that reduces the computational cost of convolution by selectively omitting multiplications whose contributions to the final sum are negligible. The core idea is to determine whether a sum of two products,  $P_1 + P_2$ , with  $P_1 \geq P_2$ , can be approximated by either  $P_1$  or  $P_2$  alone while ensuring that the resulting error remains below a user-defined threshold. Crucially, this decision is made without explicitly computing either product. By avoiding the multiplication associated with the less significant term, the overall number of MAC operations is reduced. The proposed method relies exclusively on inexpensive hardware operations, enabling efficient implementation. The approximation is based on the observation that the position of the most significant bit (MSB) in an integer’s binary representation provides an approximation of its base-2 logarithm; specifically, it equals the integer part of  $\log_2(x)$ .

Intuitively, the most significant bit (MSB) indicates the highest power of two that fits within a number, which directly reflects the number’s order of magnitude in base 2. Any positive integer  $x$  can be expressed as  $x = 2^k + r$ , where  $2^k$  is the largest power of two not exceeding  $x$  and  $0 \leq r < 2^k$ . The position of the MSB corresponds to this exponent  $k$ , meaning that  $MSB(x) = k$ . Taking the base-2 logarithm yields  $k \leq \log_2(x) < k+1$ , so the MSB position is exactly the integer part of  $\log_2(x)$ . Thus, the position of the MSB serves as a simple, hardware-friendly proxy for the logarithmic magnitude of a number. For a product of two values, the MSB position of the result is approximately the sum of the MSB positions of the operands. Consequently, relative magnitudes of products can be compared by examining only sum of MSB positions, without performing multiplication. Let the MSB position of a value  $x$  be denoted as  $M(x)$ . For two products  $P_1 = a \cdot b$  and  $P_2 = c \cdot d$ , define

$$\Delta = (MSB(a) + MSB(b)) - (MSB(c) + MSB(d))$$

If  $\Delta \geq T$ , for a predefined threshold  $T$ , then  $P_1$  is considered the dominant term and  $P_2$  can be omitted from the computation. MSB extraction and comparison are low-cost hardware operations, making this decision mechanism highly efficient. To illustrate the method, consider approximating  $P_1 + P_2$  as  $P_1$  under the constraint that  $P_2$  contributes no more than 1% of  $P_1$ :

$$\frac{P_2}{P_1} \leq 0.01$$

Taking logarithms yields

$$\log_2(P_1) - \log_2(P_2) \geq \log_2(100) \approx 6.64$$

Since  $MSB(x) \approx \log_2(x)$ , this condition can be conservatively approximated using MSB positions as

$$(MSB(a) + MSB(b)) - (MSB(c) + MSB(d)) \geq 7$$

When this inequality holds, the approximation is applied, requiring only one multiplication instead of two multiplications and one addition. This approximation technique can eliminate a substantial number of multiplications in common convolution scenarios. In convolutional neural networks (CNNs), the resulting approximation error has minimal impact on inference accuracy provided that the extracted features remain sufficiently distinguishable. For example, a convolution with a  $3 \times 3$  filter computes an output of the form

$$Y = \sum_{i=1}^9 w_i \cdot x_i$$

where  $w_i$  are filter coefficients and  $x_i$  are input values. In the worst case, the theoretical maximum error introduced by the proposed approximation is eight times the maximum allowed error of a single omitted product. However, as demonstrated in later sections, empirical results show that the actual error in practical applications is typically much smaller.

*Pseudocode: MSB-Based Approximation for  $n$  Products*

- **Input:** Sets of operands  $\{(a_1, b_1), (a_2, b_2), \dots, (a_n, b_n)\}$ , Threshold  $T$
- **Output:** Approximated sum  $S \approx \sum_{i=1}^n (a_i \times b_i)$
- **Step 1: Compute MSB Magnitudes**
  - **for** each pair  $(a_i, b_i)$  **do**:
  - \*  $MSB_i \leftarrow MSB(a_i) + MSB(b_i)$
- **Step 2: Identify Dominant Magnitude**
  - $MSB_{max} \leftarrow \max(MSB_1, MSB_2, \dots, MSB_n)$
- **Step 3: Conditional Summation**
  - Initialize  $S \leftarrow 0$
  - **for**  $i = 1$  **to**  $n$  **do**:
  - \* **if**  $(MSB_{max} - MSB_i) < T$  **then**:
  - $S \leftarrow S + (a_i \times b_i)$  // Include significant product
  - \* **else**:
  - // Skip multiplication:  $P_i$  is negligible
- **return**  $S$

#### IV. HARDWARE IMPLEMENTATION

This section describes how a hardware implementation of the above algorithm was done to perform `conv_approx()` operation specifically for input matrices of dimensions  $4 \times 4$  and filter matrices of size  $3 \times 3$  to test hardware feasibility. This operation is then iteratively called using inline C commands to perform convolution for larger input matrices. To test effect of the approximation on the output of CNNs and as preliminary error analysis, `conv_approx()` function was used to perform convolutions during inference of an MNIST image using LeNet-Accel model as described by [18]. More thorough error, accuracy and performance analysis is described in subsequent sections.

#### A. Baseline Processor and Integration Strategy

RISC-V is an open, modular instruction-set architecture built around a simple RISC-style base ISA, with a clean and extensible structure that separates a small mandatory core from optional standard extensions and reserved opcode spaces for customization, allowing designers to add application-specific instructions while remaining compatible with existing tools and software. The RISC-V core is a high-performance 32-bit RISC-V processor developed for the PULPino SoC within the Parallel Ultra-Low Power (PULP) platform, featuring a 4-stage in-order pipeline and full support for the RV32IMFC ISA, including integer multiplication, compressed instructions, and single-precision floating-point operations. In this work, one of the four currently unused opcodes, `0x77`, is repurposed to define a custom `conv_approx()` instruction, which is implemented through a custom hardware block integrated into the processor's execute stage. This block interfaces directly with the instruction decoder to receive control signals and with the register file to access source operands, allowing the decoder to activate the specialized logic when the custom opcode is detected and to forward results through the standard write-back path, while its connection to pipeline flow-control signals ensures correct synchronization with the core's normal execution and memory access cycles.

#### B. Custom Instruction Encoding and Execution Model

The function `conv_approx()` uses inline RISC-V assembly to invoke a custom hardware instruction. The function is a R-type instruction encoded with opcode `0x77` via the `.insn` directive, the input register `rs1` is used to store the size of the input array and the input register `rs2` is used to store the starting address of the input array. The custom instruction consumes the two input registers holding address and size, performs some accelerator-defined operation which is elaborated in the next section, and writes its result into the output register `result`, which is mapped back to a C variable. The `__volatile__` qualifier prevents the compiler from reordering or removing the instruction, ensuring the custom operation is executed exactly as written.

#### C. Hardware Architecture of the Approximate Convolution Unit

A 5-stage Finite State Machine (FSM) in the accelerator module implements the `conv_approx()` operation between an input  $4 \times 4$  matrix and a  $3 \times 3$  kernel matrix. The 9 elements of the kernel matrix are stored in the acceleration module, and each of their MSB locations is pre-computed and stored. The states of the FSM are `IDLE`, `GET_DATA`, `STAGE_1`, `STAGE_2`, `STAGE_3`, and `DONE`.

**IDLE:** The FSM starts here, signaling it is ready to accept a new command. It monitors the input for a convolution operation signal, at which point it captures the execution parameters before transitioning to data acquisition.

**GET\_DATA:** In this state, the FSM activates data fetching to fill its internal buffers. It stays in this loop until the required amount of data is retrieved from memory, ensuring the  $4 \times 4$  data window is fully populated before beginning calculations.

**STAGE\_1 (MSB Analysis):** This stage computes MSB locations of the 16 input values ( $x_{i,j}$ ). Negative values are converted to two’s complement and processed by a priority-encoder-like structure that extracts the MSB position of each 32-bit value as a 5-bit quantity. MSB locations are obtained for both inputs  $MSB(x_i)$  and filter coefficients  $MSB(w_i)$ .

**STAGE\_2 (Pruning and Multiplication):** This stage performs the core optimization. For each output,

$$MSB_{\max} = \max(MSB(x_i) + MSB(w_i))$$

is computed using a combinational reduction tree. A partial product

$$P_i = x_i \cdot w_i$$

is evaluated only if

$$MSB(x_i) + MSB(w_i) + T \geq MSB_{\max},$$

where  $T$  is a tunable threshold; otherwise, the product is suppressed.

**STAGE\_3 (Accumulation):** The FSM sums the retained partial products for each convolution window to produce the final outputs ( $y_0, y_1, y_2, y_3$ ).

**DONE:** The FSM asserts completion flags and waits for external acknowledgment before resetting internal state and returning to IDLE.

TABLE II: Area, Power and Delay analysis using 65nm tech

Metric	MSB-based Pruning Block	% Increase w.r.t. RISCY
Area ( $\mu\text{m}^2$ )	180050.68	108.23%
Power (mW)	0.849	11.50%
Delay (ns)	2.81	0%

#### D. Preliminary Error Analysis on inference using LeNet-Accel

Following is the numerical comparison of the output of LeNet-Accel when done using standard convolution and using `conv_approx()`. The tunable threshold has been set to approximate products which are less than 1% of the largest product. The mean absolute error percentage is 0.97% and the median absolute error percentage is 0.65%. Errors are  $\leq 1\%$  except for two low magnitude outliers making them more susceptible to percentage changes. We see that it is extremely unlikely for the inference to change due to this approximation being performed at this threshold. More thorough analysis is performed in the subsequent section.

TABLE III: Comparison of Exact and Custom Block Outputs

Exact Output	Custom Output	Abs. Error	Percentage Error
-3077	-3073	4	0.13%
-2351	-2357	6	0.26%
-8059	-8122	63	0.78%
-2502	-2524	22	0.88%
-5111	-5137	26	0.51%
6537	6632	95	1.45%
-2352	-2360	8	0.34%
8202	8270	68	0.83%
-1345	-1400	55	4.09%
16139	16206	67	0.41%

## V. ERROR ANALYSIS AND RESULTS

We first perform the `conv_approx()` operation on individual MNIST images with various filters to examine output, error and performance with varying thresholds of approximation. Then, we perform inference on LeNet-5 model trained on MNIST dataset where all convolutions are performed using `conv_approx()` and analyse accuracy vs number of MACs vs error threshold.

### A. MNIST

The MNIST dataset (Modified National Institute of Standards and Technology) is a massive collection of 70,000 small, grayscale images of handwritten digits from 0 through 9. It is widely considered the ‘‘Hello World’’ of machine learning because it provides a standardized way to train and test computer vision models. Each image is a  $28 \times 28$  pixel square, and the dataset is split into a training set of 60,000 images and a test set of 10,000 images. Since the optimization achieved by sparsity-dependent paradigms such as `conv_approx()` depends on the sparsity of the input dataset, the following table summarizes key statistics of MNIST.

TABLE IV: Statistics of MNIST dataset

Statistic	Value
Pixels per image	784
Average zero pixels per image	633.92
Minimum zero pixels per image	433
Maximum zero pixels per image	750
Standard deviation (zero pixels)	41.46
Overall zero-pixel percentage	80.86%
Mean	$\approx 33.3$
Standard deviation	$\approx 78.6$

In the following image, we demonstrate the visualization of outputs produced by exact convolution and by `conv_approx()` under different approximation thresholds. Even for relatively large thresholds, the visual features of the output remain largely indistinguishable. This is achieved while realizing a 62.76% reduction in the number of multiplications relative to hard zero-skipping approaches and a 96.44% reduction relative to exact convolution.

TABLE V: Average Number of Multiplications per Image

Configuration	Avg. Multiplications
Exact Convolution	6084
Non-Zero Multiplications	1354.0214
Threshold = 0.03	1256.661
Threshold = 0.06	1167.6030
Threshold = 0.10	1032.2543
Threshold = 0.25	506.2085

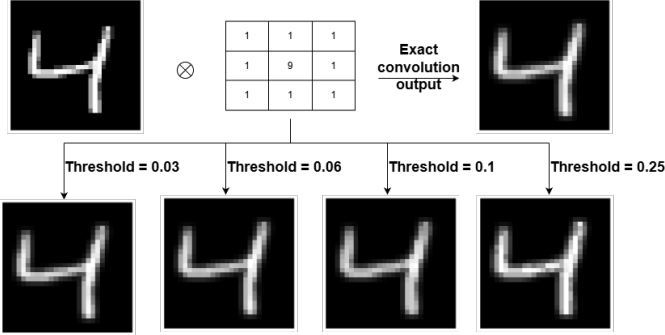


Fig. 2: Visual demonstration of outputs with different error thresholds.

While the `conv_approx()` operator may not be suitable for applications requiring an exact output, CNNs only require distinguishing between spatial patterns. Also, subsequent feature maps produce numerous small positive values which existing paradigms are forced to multiply which `conv_approx()` can skip. This makes `conv_approx()` highly suitable during inference of CNNs. We examine the results of `conv_approx()` during inference of LeNet-5 in the next section.

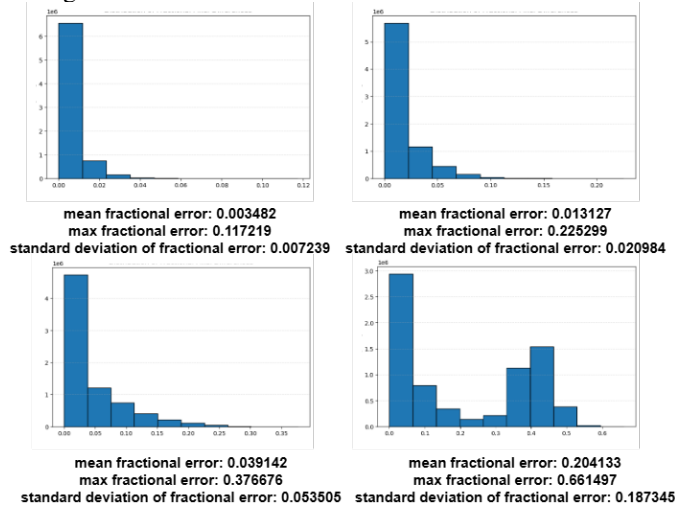


Fig. 3: Distribution of fractional pixel errors for each of the four error thresholds. top left(T = 0.03),top right(T = 0.06), bottom left(T = 0.1), bottom right(T = 0.25).

### B. LeNet-5

LeNet-5 is a classic convolution neural network composed of three convolution stages followed by two fully connected layers and a 10-class output. The first convolution layer (C1) applies 6 filters of size  $5 \times 5$  to a single-channel input image, producing 6 feature maps that capture low-level patterns. The second convolution layer (C3) uses 16 filters of size

$5 \times 5$  operating across the 6 C1 feature maps to learn more complex, spatially distributed features. The third convolution layer (C5) applies 120 filters of size  $4 \times 4$  over the 16 C3 maps, effectively collapsing the spatial dimensions and yielding a 120-dimensional feature vector. This representation is fed into a fully connected layer F6 with 84 neurons to perform high-level feature abstraction, followed by a final fully connected output layer that maps the 84 features to 10 class scores, typically corresponding to digit classes in MNIST.

The sparsity in subsequent feature maps is dependent on the kind of activation function used. ReLU forces all negative values of the feature maps to 0, thus generating significant fractions of 0 values as analyzed in table. Other smooth activation functions such as tanh generate no 0 values in subsequent feature maps, thereby restricting traditional sparsity exploiting paradigms to the ReLU activation function. Much of the non-zero values in these feature maps are small in magnitude, thereby making `conv_approx()` suitable to skip significant number of multiplications.

Table IV: Sparsity Statistics for ReLU LeNet-5 Model

Layer	Avg (%)	Min (%)	Max (%)	StdDev (%)
C1	45.11	38.43	54.11	2.52
S2	36.00	30.56	45.60	1.70
C3	50.25	44.73	56.25	1.58
S4	27.38	16.80	42.19	3.40
C5	55.10	41.67	65.00	3.45
F6	48.19	33.33	63.10	4.04

We have analysed accuracy vs number of MAC operations vs threshold for LeNet using both tanh and ReLU activation. From the analysis, we can see that using ReLU activation and at no loss of accuracy, inference is performed while having to compute on average only 11.58% of the total multiplications which translates to having to compute on average 17.79% of the non-zero multiplications in convolutional layers. While using smoother activation functions like tanh, this translates to having to perform on average 25.13% of total multiplications which translates to 33.17% of non-zero multiplications at no loss of inference accuracy.

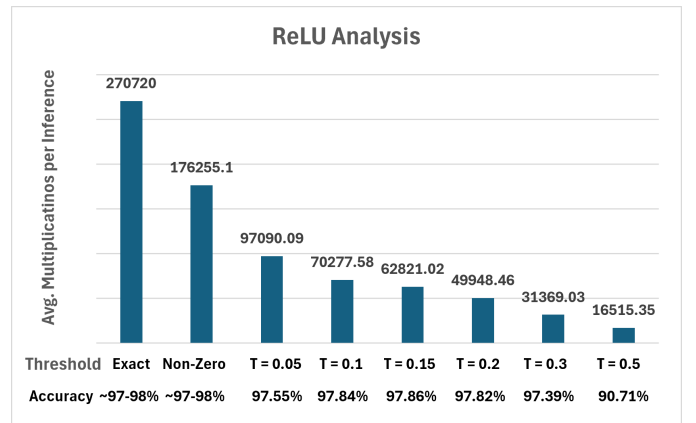


Fig. 4: At T=0.3, 11.58% of total MACs preserve accuracy.

TABLE VI: Impact of Different Thresholds on Convolution Multiplications and Accuracy for Tanh and ReLU Activations

Layer	Exact Convolution	Non-Zero Multiplications	Threshold						
			0.05	0.1	0.15	0.2	0.3	0.5	
Tanh	conv_layer_1	86400	20778.3	17964.25	16068.44	14829.27	12897.59	10537.48	7025.00
	conv_layer_2	153600	153600.0	93101.69	74078.25	54322.51	45489.36	27699.23	12618.12
	conv_layer_3	30720	30720.0	21629.76	16415.36	12688.72	9648.98	5552.83	1767.59
	<b>Average MACs per Inference Accuracy</b>	270720 ~97-98%	205098.3 97-98%	132695.7 97.96%	106562.05 97.53%	81840.5 96.88%	68035.93 97.62%	43789.54 91.64%	21410.71 61.38%
ReLU	conv_layer_1	86400	20778.3	17574.59	15637.01	14278.06	12234.10	10372.30	6988.47
	conv_layer_2	153600	130788.0	66094.82	45949.18	42637.36	33567.69	17951.35	8410.60
	conv_layer_3	30720	24688.8	13420.68	8691.39	5905.60	4146.67	3045.38	1116.28
	<b>Average MACs per Inference Accuracy</b>	270720 ~97-98%	176255.1 ~97-98%	97090.09 97.55%	70277.58 97.84%	62821.02 97.86%	49948.46 97.82%	31369.03 97.39%	16515.35 90.71%

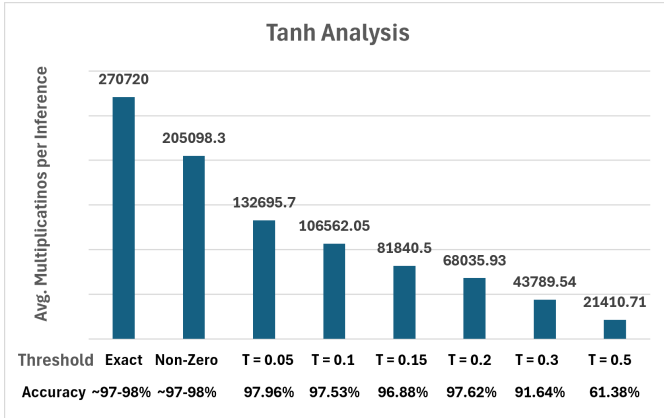


Fig. 5: At T=0.2, 25.13% of total MACs preserve accuracy.

## VI. CONCLUSION

We have demonstrated that using this novel approximation algorithm, LeNet-5 inference can be performed at no accuracy loss while achieving an 88.42% and 74.87% reduction in MAC operations for ReLU and Tanh implementations respectively. This in turn will lead to reduction in power consumed by clock gating of the multipliers when a product term need not be multiplied. As emphasized in the introduction, This power reduction will be sub-linear to the reduction in the number of MACs as in prior research, it has been established that in newer technologies memory access is the dominant consumer of power which cannot be avoided. MAC operations have been quoted to consume a fraction of between 0.3 to 0.5 of the power consumption during inference according to various sources listed in the introduction. Assuming a conservative fraction of 0.4, the reduction in MAC operations will result in reduction of power consumption by approximately  $0.4 * 0.88 = 35.2%$  and  $0.4 * 0.74 = 29.96%$  for ReLU and Tanh activation respectively.

## REFERENCES

- [1] S. Han et al., "EIE: Efficient inference engine on compressed deep neural network," in *Proc. 43rd Annu. Int. Symp. Comput. Archit. (ISCA)*, 2016.
- [2] A. Mishra et al., "Accelerating sparse deep neural networks," *NVIDIA Technical Blog*, 2021.
- [3] L. Deng et al., "Model compression and hardware acceleration for neural networks: A comprehensive survey," *Proc. IEEE*, 2020.
- [4] J. Albericio et al., "Cnvlutin: Ineffectual-neuron-free deep neural network computing," in *Proc. 43rd Annu. Int. Symp. Comput. Archit. (ISCA)*, 2016.
- [5] A. Aimar et al., "Nullhop: A flexible convolutional neural network accelerator based on sparse representations of feature maps," *IEEE Trans. Neural Netw. Learn. Syst. (TNNLS)*, 2018.
- [6] P. Judd et al., "Stripes: Bit-serial deep neural network computing," in *Proc. 49th Annu. IEEE/ACM Int. Symp. Microarchitecture (MICRO)*, 2016.
- [7] J. Albericio et al., "Bit-pragmatic deep neural network computing," in *Proc. 50th Annu. IEEE/ACM Int. Symp. Microarchitecture (MICRO)*, 2017.
- [8] S. Hooker et al., "The hardware lottery," *Commun. ACM*, 2020.
- [9] Z. Zhang et al., "Sparch: Efficiently exploiting broad sparsity in DNNs," in *Proc. IEEE Int. Symp. High-Performance Comput. Archit. (HPCA)*, 2020.
- [10] Y.-H. Chen, T. Krishna, J. Emer, and V. Sze, "Eyeriss: An energy-efficient reconfigurable accelerator for deep convolutional neural networks," in *IEEE Int. Solid-State Circuits Conf. (ISSCC) Dig. Tech. Papers*, 2016, pp. 262-263.
- [11] V. Akhlaghi et al., "SnaPEA: Predictive early activation for reducing computation in deep convolutional neural networks," in *Proc. 45th Annu. Int. Symp. Comput. Archit. (ISCA)*, 2018.
- [12] K. He, X. Zhang, S. Ren, and J. Sun, "Deep residual learning for image recognition," in *Proc. IEEE Conf. Comput. Vis. Pattern Recognit. (CVPR)*, 2016, pp. 770-778.
- [13] A. Krizhevsky, I. Sutskever, and G. E. Hinton, "ImageNet classification with deep convolutional neural networks," *Commun. ACM*, vol. 60, no. 6, pp. 84-90, 2012.
- [14] C. Szegedy et al., "Going deeper with convolutions," in *Proc. IEEE Conf. Comput. Vis. Pattern Recognit. (CVPR)*, 2015, pp. 1-9.
- [15] Zhang et al., "Cambricon-X: An accelerator for sparse neural networks," 2016.
- [16] K. Guo et al., "RRAM based buffer design for energy efficient CNN accelerator," in *Proc. IEEE Comput. Soc. Annu. Symp. VLSI (ISVLSI)*, 2018.
- [17] S. Zhang et al., "Cambricon-X: An accelerator for sparse neural networks," in *Proc. 49th Annu. IEEE/ACM Int. Symp. Microarchitecture (MICRO)*, 2016, pp. 1-12.
- [18] S. Wang et al., "Optimizing CNN computation using RISC-V custom instruction sets for edge platforms," *IEEE Trans. Comput.*, vol. 73, no. 5, pp. 1371-1384, May 2024.